Praise Worthy Prize

International Review on Modelling and Simulations (I.RE.MO.S.), Vol. 7, N. 4
ISSN 1974-9821 *August 2014*

An Energy Management Strategy for Fuel-cell Hybrid Electric Vehicles via Particle Swarm Optimization Approach

A. Del Pizzo, S. Meo, G. Brando, A. Dannier, F. Ciancetta

Abstract – *The paper focuses on an energy management strategy for an electric vehicles powered with three power sources (PEM fuel cells, $LiFePO_4$ battery and supercapacitors). The aim of the proposed strategy is to split the power demand between the different sources maximizing the driving range and the performances of the vehicle and increasing the life cycle of the battery and of the PEM fuel cell.*
To accomplish load sharing an energetic model of the overall system based on experimentally validated models of the PEM Fuel Cell, $LiFePO_4$ battery and supercapacitors is formulated and an optimal control problem with inequality constraints is resolved using the particle swarm optimization technique (PSO) to search the global near-optimum at each sample interval. The results show that the proposed strategy guarantees energy saving and assures failsafe operations for the battery and the PEM Fuel Cell unaffecting the drivability of the vehicle and increasing autonomy.

Keywords: *Electric Vehicles (EV), Energy Management Strategy, Energy Storage System (ESS), Particle Swarm Optimization (PSO), Batteries, Ultracapacitors, PEM Fuel Cell*

Nomenclature

Vehicle		
m	Vehicle mass	[kg]
A	Vehicle frontal area	[m^2]
C_d	Air drag coefficient	
C_r	Rolling resistance	
ρ	Air density	[kg/m^3]
g	Gravity	[m/s^2]
h	Road slope	
R	Vehicle wheel radius	[m]
F_r	Final drive ratio	
G_r	Gear ratio	
v	Vehicle linear speed	[m/s]
n_w	Vehicle-wheels angular speed	[rpm]
P_D	Required propulsion power	[kW]
Battery and Fuel Cell:		
U_B	Open-circuit battery voltage	[V]
R_B	Battery equivalent circuit resistance	[Ω]
E_{B0}	Battery rated energy	[Wh]
E_B	Battery energy level	[Wh]
SOC_B	Battery State of Charge	[%]
P_B	Battery power (with losses)	[kW]
P_{SB}	Battery storage power (without losses)	[kW]
$P_{B,loss}$	Battery losses	
η_B	Battery efficiency	
P_{Fc}	Fuel-cell power (with losses)	[kW]
P_{SFc}	Fuel-cell storage power (without losses)	[kW]
η_{Fc}	Fuel-cell efficiency	
Ultracapacitors		
U_C	Open-circuit ultracapacitor voltage	[V]
R_C	Ultracapacitor equivalent circuit resistance	[Ω]
E_{C0}	Ultracapacitor rated energy	[Wh]
E_C	Ultracapacitor energy level	[Wh]
SOC_C	Ultracapacitor State of Charge	[%]
P_C	Battery power (with losses)	[kW]
P_{SC}	Battery storage power (without losses)	[kW]
$P_{C,loss}$	Battery losses	[kW]
η_C	Ultracapacitor efficiency	
Electrical loads:		
P_L	Required on-board electrical loads power	[kW]
Electric motor:		
P_M	Mechanical power of the electric motor	[kW]
P_E	Electrical power of the electric motor	[kW]
n_e	Angular speed of electric motor	[rpm]
η_e	Electric motor efficiency	
PSO algorithm:		
J	Cost function	
$\mathbf{v}_i^k$	The velocity of the particle i at step k	
$\mathbf{x}_i^k$	The position of particle i at step k	

$\mathbf{p}_i^k$	The individual best candidate solution for particle i at step k
$\mathbf{p}_g^k$	the swarm's global best candidate solution at step k
χ	Constriction coefficient
c_1, c_2	Acceleration constants
$rand_1()$, $rand_2()$	Uniformly distributed random values

Simulations:

T_c	Period of the drive cycle	[s]
T_s	Sample period	[s]

Functions:

sign(x)	Signum function

I. Introduction

The fast-growing market for electric vehicles (EVs), which includes hybrids, plug-in hybrids, and battery electric vehicles, has become a small but important part of the global automotive industry. Governments worldwide are keen to see increasing penetrations of EVs due to the environmental, economic, and energy security benefits engendered by these vehicles.

In the panorama of EV a solution that ensures autonomy comparable with the internal combustion engine vehicles cannot be realized, at the present, regardless by the use on board of a fuel cells with related hydrogen tanks (FCEVs). FCEVs run on hydrogen gas rather than gasoline and emit no harmful tailpipe emissions. Several challenges must be overcome before these vehicles will be competitive with conventional vehicles (particularly the onboard hydrogen storage, the Fuel Cell durability and reliability, the vehicle costs and the safety problems) but the potential benefits of this technology are substantial.

For this reason the scientific research on the topic is growing more and more and the main auto industries of the world have fixed this decade as target for the commercialization. In January 2013, Daimler AG, Ford Motor Company and Nissan Motor Co. Ltd., under the Alliance with Renault, have signed a unique three-way agreement for the joint development of common fuel cell system. The goal of the collaboration is to jointly develop a common FCEV system while reducing investment costs associated with the engineering of the technology, and deriving efficiencies through economies of scale, helping to launch the world's first affordable, mass-market FCEVs as early as 2017.

Toyota Motor Corp. and Honda Motor Co. have also pledged to offer next-generation fuel-cell vehicles set to launch in 2015. Hyundai Motor Co. announced in November 2013 that it will begin offering a fuel-cell version of the Tucson crossover this spring, making it the first mass-market, federally certified hydrogen fuel-cell vehicle in the United States. Many concept cars have been already developed (for example Toyota FCV Concept", World Premiere at the 43rd Tokyo Motor Show 2013, the Nissan TeRRA SUV concept was unveiled at the 2012 Paris Motor Show sept. 2012, GM HydroGen4, Honda FCX Clarity and Mercedes-Benz F-Cell are all pre-commercial examples of fuel cell electric vehicles). Normally the main subsystems of such type of vehicle are the hydrogen storage tank, the fuel cells stack, the high output battery, the electric motor and the power unit (Fig. 1).

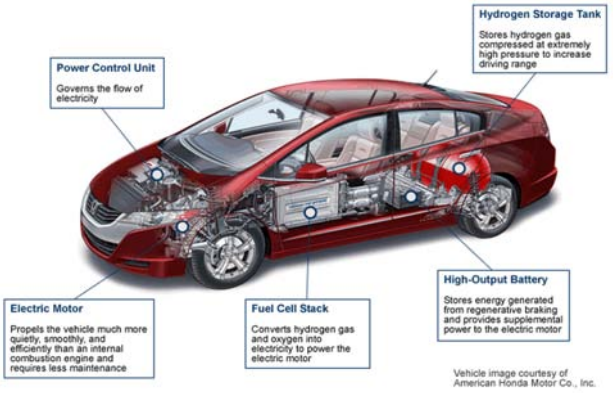

Fig. 1. Main subsystems of Fuel-cell Hybrid Electric vehicles

Generally, with this type of vehicle at a steady cruising speed, the motor is powered by the fuel cell.

When more power is needed, for example during sudden acceleration, the battery supplements the fuel cell's output. Conversely, at low speeds when less power is required, the vehicle runs on battery power alone. During deceleration the motor functions as an electric generator to capture braking energy, which is stored in the battery.

The main drawbacks of such type of solution are the slow dynamics of the fuel cells (that is partially compensated by the Li-ion battery) and the electrical limits of the Li-ion batteries. In fact, even if it is true that the new technologies of Li-ion batteries have high specific energy, superior power density and a good calendar life they present however different problems and limitations yet [1]-[4]. In particular in order to maximally utilize the battery performance the input power and output power of the cell should be managed so that the voltage should be kept within a definite range, otherwise the deterioration in performance of the cell is accelerated. Moreover if the battery temperature is high, the charging and discharging current should be restricted to reduce the temperature increase caused by internal resistance of the battery. On the other hand, at low temperature, battery charge acceptance declines, so charging current should be restricted. High rate charging current under low temperature may cause deterioration or internal short circuit induced by deposited metal lithium around negative electrode in the worst case scenario.

Therefore, the upper limits of charging current and discharging current should be kept within a definite range depending also on the temperature. In addition the efficiency of the batteries is depending on the state of the charge (SOC) and it decreases in discharging phase with

low SOC. Because of all these considerations it is interesting to evaluate in which measure an auxiliary system of energy storage can increase the performances and the efficiency of the overall FCEV vehicle. In recent years many energy storage systems have been analysed including ultracapacitor, flywheel and superconducting energy storage systems [5]. Among all these new technologies, ultracapacitors, which have higher power density, longer life cycle and an equivalent serie resistance (ESR) practically independent on the SOC appear to be one of the most promising alternatives in vehicular applications [6], [7]. Thanks to this ESS a possible energy management strategy, also adopted in this paper, can be the following: at a steady cruising speed, the motor is powered by the fuel cell. When more power is needed, for example during sudden acceleration, the ultracapacitor supplements the fuel cell's output. Conversely, at low speeds when less power is required, the vehicle runs on battery power alone. In this way ultracapacitor can extend the life of a battery and of Fuel-Cell (FC), save on replacement and maintenance costs, and enable a battery to be little downsized. At the same time, it can increase available power density by providing high peak power whenever necessary [8]-[10]. Nevertheless, in order to maximize the benefits of the adoption of a three ESS it is necessary the formalization of an energy management strategy able to maximize the advantages due to the three power source [11]-[14].

In the paper it is suggested an extension of the energy management strategy proposed by [15] that splits the vehicle power demand between Fuel cells, Li-ion battery and ultracapacitor maximizing the driving range and the performances of the vehicle and increasing the life cycle of the battery and of the Fuel cells. This strategy starting by the knowledge of the power demand (power of the drive train and of the ancillary loads) evaluates the optimal load sharing among the three power sources in order to maximize the global efficiency while protecting the battery and the FC. The ultracapacitors are deputized to preserve the life of these sources: they are enabled only if the values of battery voltage and/or the FC output current are out of a definite range.

In the paper the mathematical model of a FCEV is developed based on improved experimental models of the PEM Fuel Cell, Li-ion battery and Supercapacitor.

Then, based on particle swarm optimization technique [16]-[17], an optimal control problem with inequality constraints is formulated imposing in each interval of control the maximization of the global efficiency while protecting the other sources.

Two cases are considered (Lead-acid battery and $LiFePO_4$ battery). In each case, the performance of EV driving only with the battery as unique ESS have been compared with the performance of EV driving with the same battery added to the UC and the FC, controlled by the proposed PSO energy management strategy.

The numerical results show the goodness of the proposal and will be presented and discussed in the next sections.

II. Modelling of FCEV

II.1. Basic Assumptions

The following assumptions are made:

- The sampling interval of the control strategy is sufficiently large (1 s or larger) so that to neglect the dynamic behavior of the different dispositive (electric motor, converters, sources and so on): their characteristics can be represented by static models.
- The weight of the energy storage system for all the considered type of batteries (Lead-acid battery and LiFePO4 battery) is always near to the 10% of the empty vehicle weight.
- The control strategy guarantees that the drivability of the vehicle remains unaffected, therefore at each time instant the drive train power, as well as the vehicle speed, are known.
- The power request from the electric loads is assigned.

Fig. 2 shows a power flow diagram of the vehicle. A multi-input bidirectional DC/DC converter realizes the power split [18].

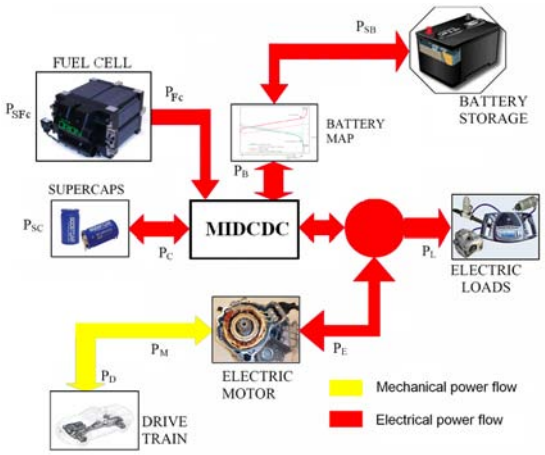

Fig. 2. Power flow diagram of PEV

II.2. Electric Motor

The considered propulsion motor is a PM brushless motor, providing 47 kW. It is hypothesized that the efficiency of the electric motor is related to the mechanical power (P_M) and to the motor speed (n_e) by a nonlinear, memoryless function (static map):

$$\begin{cases} \eta_e = f_e\left(P_M, n_e\right) \\ P_M = P_E \eta_e^{sign(P_E)} \end{cases} \quad (1)$$

Fig. 3 shows the efficiency map of the brushless motor, as function of the input electric power and of the motor speed [19].

II.3. Power Train

The power P_D needed for propulsion is related to the vehicle velocity v, acceleration $\dot{v}$ and road slope h as

follows:

$$P_D(t) = f_d\left[v(t), \dot{v}(t), h(t)\right] \quad (2)$$

The function f_d includes aerodynamic and rolling losses, acceleration power and the power related to change the vehicle's altitude. This relationship is typically expressed as follows:

$$f_d(v,\dot{v},h) = \left[m\dot{v} + \frac{1}{2}\rho C_d A v^2 + mg\left(C_r + \frac{h}{100}\right)\right] v \quad (3)$$

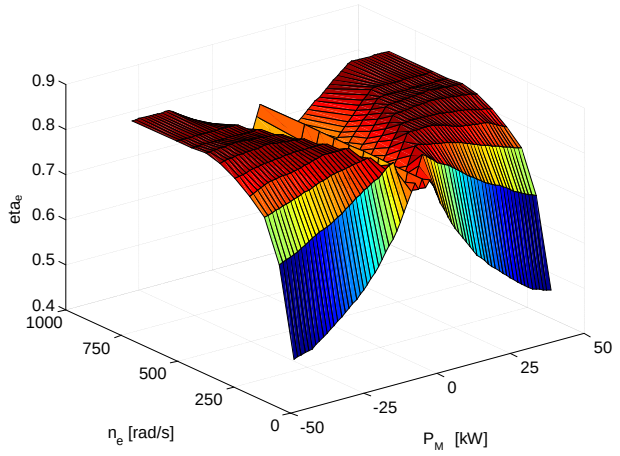

Fig. 3. The two-quadrant efficiency map of the electric motor

II.4. Battery

Many modelling of batteries have been proposed in literature [20]-[22].

In the following, for the aims of our research it is considered sufficient to adopt a modeling constituted by a voltage source U_B controlled by the output current i_b and its state of charge (SOC_B), with one resistance in series R_B. In particular, the voltage U_B and the resistance R_B are given by polynomial expressions of current and state of charge:

$$U_B = \sum_{k=1}^{4} SOC_B^{k-1} \sum_{h=1}^{2} a_{hk}\, i_B^{h-1} \quad (4)$$

$$R_B = \sum_{h=1}^{2} b_h SOC_B^h \quad (5)$$

a_{ij} are the coefficients of two 2×4 matrixes, one for charge and one for discharge operations; these are dependent on the kind of batteries used.

In the next a Winston $LiFePO_4$ battery, model WB-L YP40AHA, 40Ah - 3.2 TI, has been considered. Model parameters are obtained experimentally by means of a series of charge/discharge cyc1es, monitoring the terminal voltages and currents at controlled temperature [23]. The cell is charged with a square wave current with amplitude 40 A (lC), period 16 min and duty cycle 6 min; so that after 10 periods the SOC is 100%, as shown in Fig. 4; starting from a complete state of charge the battery is discharged with a square wave current with amplitude 40 A (1 C), period 16 min and duty cyc1e 6 min, so that after 10 periods the SOC is 0%.

All the relative maximum values of voltage reached during the discharge pauses, and all the relative minimum values reached during the charge pauses, are re-elaborated by means of a polynomial interpolation that allows to construct the numerical function U_B (SOC) as shown in Fig. 4.

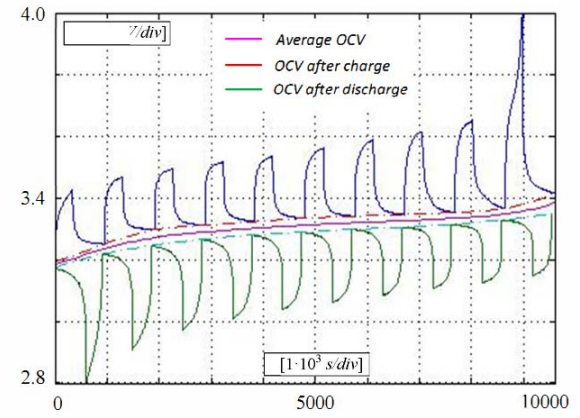

Fig. 4. Behaviour of the OCV during charge and discharge phases

In Fig. 5 the resistance R_B in charge (R_c) and discharge (R_d) phases as a function of SOC are reported.

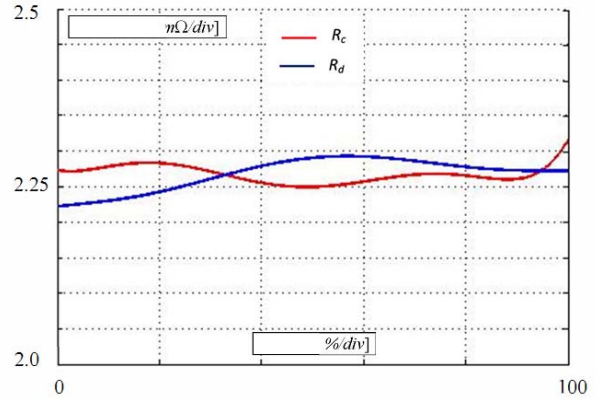

Fig. 5. Equivalent resistance of the battery in charge and discharge phases vs %SOC

The power P_B in input or in output from the battery is the algebraic addition of the power P_{SB} (positive in charging mode, negative in discharging mode) actually stored in the battery and the battery losses that are supposed like a polynomial (quadratic) function of P_{SB}, and are positive for both charging and discharging conditions:

$$P_B = P_{SB} + P_{B,loss} \quad (6)$$

$$P_{B,loss} = \beta_B P_{SB}^2 \tag{7}$$

with:

$$\beta_B = \frac{R_B}{U_B^2} \tag{8}$$

The battery energy level E_B is given by:

$$E_B(t) = E_B(0) + \int_0^t P_{SB}(\tau)\, d\tau \tag{9}$$

The state of charge (SOC_B) is defined as:

$$SOC_B(t) = \frac{E_B(t)}{E_{B0}} \tag{10}$$

where E_{B0} is the battery rated energy.

The efficiency of the battery is defined as:

$$\eta_B = \left(\frac{P_{SB}}{P_B} \right)^{sign(P_B)} \tag{11}$$

The modeling is completely assigned if R_B in charging and discharging mode and U_B are assigned over all the SOC range [19] and the efficiency of the $LiFePO_4$ battery versus the P_B parameterized respect to the SOC, obtained with the depicted modeling, can be easily achieved.

Fig. 6 shows a photo of the considered $LiFePO_4$ battery stack.

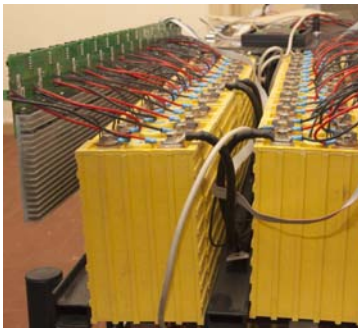

Fig. 6. Photo of the considered LiFePO4 battery stack

II.5. Fuel Cells

The fuel cell is an electrochemical device that converts chemical energy directly into electrical energy. With respect to internal combustion engines, fuel cell has higher energy storage capability thus enhancing the range of operation for automobile and it is a cleaner source of energy. Fuel cell also has the further advantage of using hydrogen as fuel that could reduce world's dependence on nonrenewable hydrocarbon sources.

The PEM (Polymer Electrolyte Membrane) fuel cell basically requires hydrogen and oxygen as reactants, though the oxidant may also be ambient air, and these gasses must be humidified to prevent membrane dehydration [24]-[25]. Each single cell produces about 0.6 V and can be combined in a fuel cell stack to obtain the required electrical voltage and power.

The operating temperature is in the range of 70 – 100° C. One of the main weak points of the fuel cell is its slow dynamics. In fact, the dynamics of fuel cell is limited by several phenomena, as the resistance variation of the membrane, due to the temperature, or the hydrogen delivery system itself, which can introduce delays due to the pumps, the valves, and in some cases to the reforming process. Many dynamic FC models are present in literature [26]-[28]; they describe FC function, flow gasses, reforming, etc.

These models need chemical-physic-electrical parameters that are not usually provided by factories in order to preserve design patent.

In the next the dynamic FC model proposed by [29] has been adopted and validated using measurements obtained by a FC measurement system shown in Fig. 7 [30]. The electric load at the fuel cell output was implemented using the Agilent N3301A mainframe, with two N3302A electronic load modules. Each module has a current range of 0-30 A, a voltage range of 0-60 V.

This system allows constant current, constant voltage, constant resistance and transient conditions to be implemented. The electronic load allows both current and voltage to be measured by the PC during the tests, by means of the IEEE 488 interface.

The experimental characteristics of the efficiency and of the output power versus current of a single fuel cell are shown in Fig. 8 and Fig. 9.

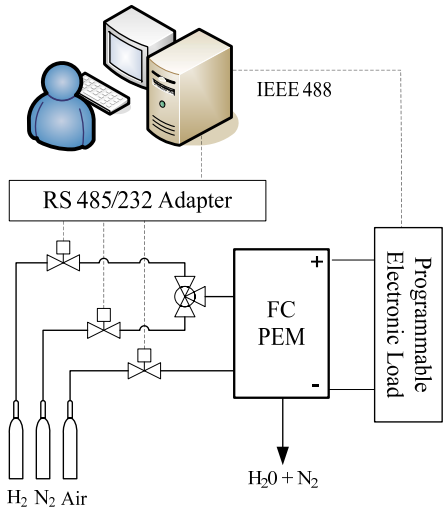

Fig. 7. Fuel Cell measurement system

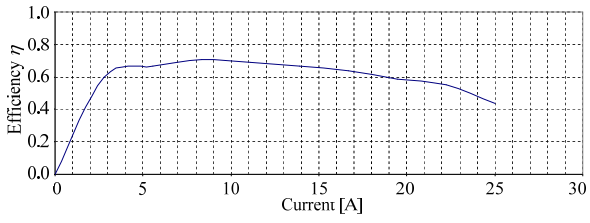

Fig. 8. Experimental efficiency diagram of the fuel cell

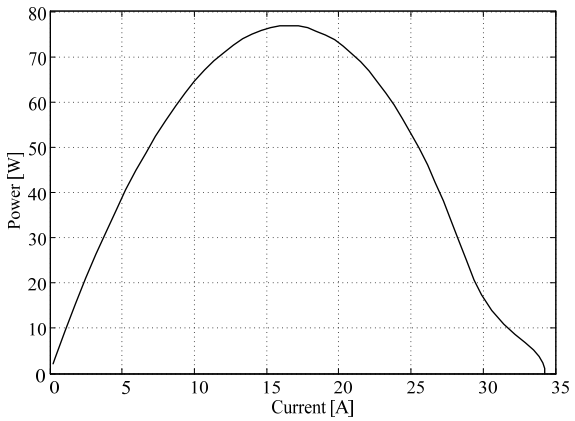

Fig. 9. Experimental output power diagram of the fuel cell

Starting by these characteristics the efficiency versus the output power $\eta_{Fc}(P_{Fc})$ of the considered FC stack has been evaluated and adequately scaled in power.

The adopted PEM fuel cell model has been validated with a comparison between the acquired and the simulated voltage and current waveforms (Fig. 10).

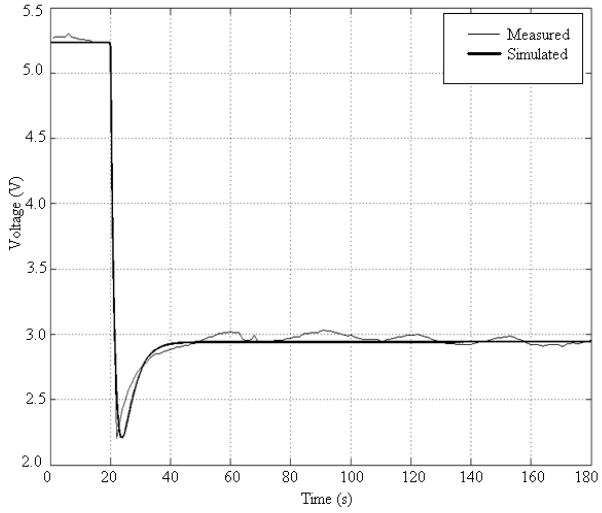

Fig. 10. Simulated and measured voltage response for 10-20 A current step variation

II.6. Ultracapacitor

In the following, the ultracapacitor (UC) has been modeled as a voltage source U_C controlled by the output current i_c and its state of charge (SOC_C), with one resistance in series R_C [31]. In particular, the voltage U_C in the following is given as follows:

$$U_C = \sqrt{\frac{2E_C}{C}} \tag{12}$$

with E_C the ultracapacitor energy level.

The power P_C in input or in output from the UC is the algebraic addition of the power P_{SC} (positive in charging mode, negative in discharging mode) actually stored in the UC and the UC losses that are like a polynomial (quadratic) function of P_{SC}, and are positive for both charging and discharging conditions:

$$P_C = P_{SC} + P_{C,loss} \tag{13}$$

$$P_{C,loss} = \beta_C P_{SC}^2 \tag{14}$$

with:

$$\beta_C = \frac{R_C}{U_C^2} \tag{15}$$

The UC energy level E_C is given by:

$$E_C(t) = E_C(0) + \int_0^t P_{SC}(\tau)\, d\tau \tag{16}$$

The state of charge is defined as:

$$SOC_C(t) = \frac{E_C(t)}{E_{C0}} \tag{17}$$

where E_{C0} is the ultracapacitor rated energy. The efficiency of the UC is defined as:

$$\eta_C = \left(\frac{P_{SC}}{P_C}\right)^{sign(P_C)} \tag{18}$$

II.7. On-board Electrical Loads

The electric power profile adopted for modeling the on-board electrical loads has been computed with a suitable software tool [32]. Such technique generates, by means of a stochastic approach, different sequences of loads activation and it gives, as output, a set of critical operative conditions suitable for testing the power source system.

III. The Proposed PSO-Based Energy Management Strategy

III.1. Formulation of the Energy Optimization Problem for a PEV

The aim of the proposed energy management strategy is to split the required power for the propulsion and the electrical loads among the electrical sources available, in order to maximize the global efficiency of the Energy Storage System (ESS), protecting the battery and the FC and unaffecting the drivability of the vehicle.

The lifetime of the battery depends on several parameters, like temperature, number of peak currents, charge and discharge cycles, etc.. To simplify, only the numbers of charge and discharge cycles and the peak currents are taken into account.

For the FC only the peak currents are taken into account. As objective function of the optimization problem, the equivalent efficiency of the ESS could be adopted. Since the main scope of the control is the maximization of the ESS efficiency, all the variables that are necessary to evaluate these quantities should be included in the objective function, with the relative constraints.

However, based on the requirements of the electrical self-sustainability, the variations in the stored electrical energy (or state-of-charge, SOC) of both the electrical sources should be taken in account as well.

Assuming these variables as the desired aims of the driver, somehow represented by the acceleration/deceleration pedal position, together with the actual values of the velocity and the propulsion power, it is possible to evaluate the objective function and to execute the optimization algorithm.

The optimization algorithm will evaluate the outputs at each sampling period on the basis of the above assumptions.

Referring to the Fig. 1, the energetic model of the vehicle in discrete time is given by the system of equations (19) (the generic quantity $f(k) \equiv f(kT_s)$), with the following conventional signs:

- $P_D > 0$ if in output from the mechanical node
- $P_E > 0$ if in output from the electrical node
- $P_B > 0$ if in output from the electrical node
- $P_C > 0$ if in output from the electrical node
- $P_{Fc} > 0$ if in input to the electrical node

$$
\begin{cases}
\left.\begin{aligned} P_M(k) &= -P_D(k) \\ n_e(k) &= F_r \cdot n_w(k) \end{aligned}\right\}(\text{mech. node}) \\
\Downarrow \\
\left.\begin{aligned} \eta_e(k) &= f_e\left(P_M(k), n_e(k)\right) \\ P_E(k) &= \frac{P_M(k)}{\eta_e^{sign(P_E(k))}} \end{aligned}\right\}(\text{electric motor}) \\
\Downarrow \\
\begin{aligned} &P_C(k) + P_B(k) + P_{Fc}(k) = \\ &= -\left(P_L(k) + P_E(k)\right) \end{aligned} \quad (\text{elec. node}) \\
\Downarrow \\
\left.\begin{aligned} \eta_B(k) &= f_b\left(P_B(k), SOC_B(k)\right) \\ P_{SB}(k) &= P_B(k)\eta_B^{sign(P_B(k))} \end{aligned}\right\}(\text{battery}) \\
\left.\begin{aligned} \eta_C(k) &= f_c\left(P_{SC}(k), SOC_C(k)\right) \\ P_C(k) &= \frac{P_{SC}(k)}{\eta_C^{sign(P_{SC}(k))}} \end{aligned}\right\}(\text{supercaps}) \\
P_{Fc} = \eta_{Fc} P_{SFc} \qquad (Fuel-cells)
\end{cases}
\tag{19}
$$

In discrete time, if we consider the battery power P_{SB} and the supercapacitor power P_{SC} as the mean value held from k to k+1, also the *SOC* is known at istant k+1:

$$SOC_B(k+1) = \frac{T_s}{E_{B0}} P_{SB}(k) + SOC_B(k) \tag{20a}$$

$$SOC_C(k+1) = \frac{T_s}{E_{C0}} P_{SC}(k) + SOC_C(k) \tag{20b}$$

At instant k+1 we have only two independent variable to choice between the following: $P_{SFc}(k+1)$, $P_{SB}(k+1)$ and $P_{SC}(k+1)$; starting from $P_{SC}(k+1)$ and $P_{SFc}(k+1)$, with the knowledge of the inputs P_L and P_D, any other quantity in the system (19) can be expressed as function of this quantity.

The optimal solution can be represented at every step by the value of P_{SC} that maximizes the following cost function:

$$J = \frac{P_{Fc}}{P_{SFc}} + \left(\frac{P_B}{P_{SB}}\right)^{sign(P_B)} + \left(\frac{P_C}{P_{SC}}\right)^{sign(P_C)} \tag{21}$$

Since the ranges of the different quantities involved in the power diagram (Fig. 1) are limited by physical constraints or by engineering design, the control strategy at every step can be formulated as a nonlinear optimization problem subject to constraints. In particular, taking into account also the aim to increase the life cycle of the battery and of the FC, the following inequality constraints must be imposed:

$$P_{SB\,min} \le P_{SB} \le P_{SB\,max} \tag{22a}$$

$$P_{SC\,min} \le P_{SC} \le P_{SC\,max} \tag{22b}$$

$$SOC_{B\,min} \le SOC_B \le SOC_{B\,max} \tag{23a}$$

$$SOC_{C\,min} \le SOC_C \le SOC_{C\,max} \tag{23b}$$

$$P_{SFc\,min} \le P_{SFc} \le P_{SFc\,max} \tag{24}$$

III.2. Proposed PSO-Based Algorithm

In the proposed PSO-based algorithm, the amount of P_{SC} and P_{SFc} have been encoded as the position value for the one-dimension particles.

Each particle is considered as a potential solution of the optimization problem, since each of them represents a specific configuration of the vehicular system.

A vector of N_p different particles is generated at each step of the PSO algorithm. This is the input of the fitness function, where starting from the P_{SC} and P_{SFc} values, we calculate any other quantity of the vehicle model for different possible situations, depending on the value of

the known quantities P_D and P_L. As the efficiency of the ESS is function of these quantities (see (19)), a vector of the cost function values is generated too, at the same step. The comparison among these values establishes the optimal value and the corresponding best particle. The adopted PSO algorithm is based on the Trelea parameters set 1 [17]. The equations to be considered for updating the velocity and position of the particles are:

$$\mathbf{v}_i^{k+1} = \chi \begin{bmatrix} \mathbf{v}_i^k + c_1 rand_1(\ldots)\left(\mathbf{p}_i^k - \mathbf{x}_i^k\right) + \\ + c_2 rand_2(\ldots)\left(\mathbf{p}_g^k - \mathbf{x}_i^k\right) \end{bmatrix} \quad (25)$$

$$\mathbf{x}_i^{k+1} = \mathbf{x}_i^k + \mathbf{v}_i^{k+1} \quad (26)$$

with the following values for the parameters:

$$\chi = 0.6;\ c_1 = c_2 = 2.83$$

The optimization strategy can be summarized as follows:

a) In *acceleration mode*, when P_D is less than an appropriate threshold, the maximization of the cost function (21) is imposed with a constraint on the supercapacitor's discharge power: it is removed when P_D is greater than the same threshold. Such strategy is adopted according to the voltage and current constraints of the battery and of the FC with the aim to preserve these sources.
b) In *deceleration mode* (either braking or motored due) the electric motor works as a generator for the battery and supercapacitor recharging, by converting the vehicle kinetic energy into electrical energy: the optimal issue is to recover all the kinetic energy splitting it among the power sources, compatibily with the physical battery, supercapacitor and motor constraints.

The steps of the proposed algorithm are the following:

Step 1: specifies the lower and upper bounds of P_{SC} and of P_{SFc} outside the fitness function;
Step 2: randomly generates a population of particles. The velocity and the position of these particles are initialized according to the constraints of step1;
Step 3: the evaluation of the fitness function is performed on the initial vector of the generated particles using the components' models (see paragraph II); according to the prefixed optimization strategy, if the constraints (22)-(24) and the motor constraint are violated, a penalty is introduced into the cost evaluation;
Step 4: new velocities and new searching points are calculated using (25), (26);
Step 5: cost values are evaluated with the same fitness function for the new searching points of step 4;
Step 6: if the cost value of each particle is better than the previous *pbest*, the value is set to *pbest*. If the best *pbest* is better than *gbest*, the value is set to *gbest*. All of *gbests* are stored as candidates for the final control strategy;
Step 7: if the iteration number reaches the maximum iteration number, then go to final step, otherwise, go to Step 4;
Step 8: the last *gbest* is set to the optimum cost if it is better than the previous, within a prefixed short margin, otherwise the algorithm return to step 4.

IV. Numerical Results

In order to evaluate the goodness of the proposed PSO energy management strategy the performance of EV driving only with the battery as unique ESS have been compared with the performance of EV driving with the same battery added to the UC and with the same battery added to the UC and to the FC. In Table I the main simulations parameters are reported.

TABLE I
SIMULATION PARAMETERS

Symbol	Quantity	Value	Unit
SIMULATION TIME:			
T_c	Drive cycle length (1 cycle)	660	s
T_s	Sample time	1	s
VEHICLE:			
	Dimensions	3.4×1.5×1.6	m
m	Mass (empty vehicle)	870	kg
A	Frontal area	1.746	m^2
C_d	Air drag coefficient	0.3	
C_r	Rolling resistance coeff.	0.009	
ρ	Air density	1.2	kg/m^3
g	Gravity	9.81	m/s^2
R	Wheel radius	0.25	m
F_r	Final drive ratio	3.93	

The adopted drive cycle is the Japanese 10-15 [26] (Fig. 11).

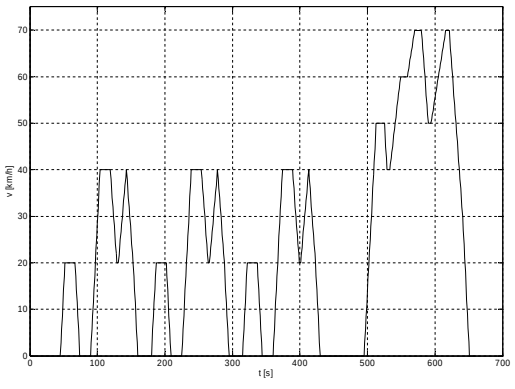

Fig. 11. Vehicle speed in the 10-15 drive cycle

The Table II reports the results of the different simulations. The row A1.1 shows the results for the case of Lead-acid battery operating as unique ESS. In this row the driving range and the specific energy consumption are reported when the Lead-acid battery starting from 80 % of SOC covers the 10-15 cycle many times until the SOC reaches the value of 10 %.

The row A1.2, shows the results for the case of dual ESS (Lead-acid battery and UC) controlled by the proposed PSO energy management strategy when the system covers the 10-15 cycle many times until the same distance of the previous case is reached. In this row the driving range, the specific energy consumption and the energy saving are reported.

The starting total energy stored in the system is equal to the starting energy stored in the previous case A1.1.

The row A1.3, shows the results for the case of three ESS (Lead-acid battery, fuel-cells and UC) controlled by the proposed PSO energy management strategy when the system covers the 10-15 cycle many times until the same distance of the previous case is reached. In this row the driving range, the specific energy consumption and the energy saving are reported.

The starting total energy stored in the system is equal to the starting energy stored in the previous case A1.1. In the rows B1.1 B1.2 and B1.3 of the Table II the same simulations of the rows A1.1, A1.2 and A1.3 have been developed but in this case the adopted battery is a $LiFePO_4$ battery.

The results of the set of the simulations show the best performance of EV driving with three ESS and controlled by the proposed energy management strategy compared with the performance of EV driving only with the battery as unique ESS.

TABLE II
SIMULATIONS RESULTS FOR THE VEHICLE WITH THREE DIFFERENT ESS TYPES (LEAD ACID, NI-MH, LI-ION), WITH AND WITHOUT ULTRACAPACITORS, WITH AND WITHOUT PROTECTION SYSTEM FOR THE BATTERY

Set/ Case	ESS Type	Drive range [km]	Specific energy consumption [Wh/km]	Energy saving [%]
A1.1	**Lead Acid Battery (85Ah)**	56.4	152	-
A1.2	**Lead Acid Battery (85Ah) + SUPERCAPS**	56.4	132.4	+13
A1.3	**Lead Acid Battery (85Ah) + SUPERCAPS + FUEL –CELLS**	56.4	129.2	+15
B1.1	**LiFePO4 battery (66Ah)**	150.5	93	-
B1.2	**LiFePO4 battery (66Ah) + SUPERCAPS**	150.5	91.4	+1.7
B1.3	**LiFePO4 battery (66Ah) + SUPERCAPS + FUEL -CELLS**	150.5	90.8	+2.4

The proposed strategy, guarantees energy saving (as consequence it increases driving range), assures failsafe operations for the battery (as consequence it increases life cycle) unaffecting the drivability of the vehicle and increasing acceleration performance.

The best solution in terms of energy saving for the considered operative conditions is the third solution.

Anyway considerable energy saving can be obtained also with only two ESS ($LiFePO_4$ battery and supercap).

To these considerations it can be added the advantage, guaranted only with the third solution, to have a life cycle saving of the FC and of the battery and a long fuel autonomy.

V. Conclusion

In this paper an extension of the PSO Based Energy Management Strategy for Pure Electric Vehicles proposed by [15] has been proposed and fully analyzed.

The suggested strategy splits the required power for the propulsion and the electrical loads among the electrical sources available (fuel-cells, battery and ultracapacitor), in order to maximize the global efficiency of the Energy Storage System, protecting the battery and unaffecting the drivability of the vehicle.

Compared with the considered type of the battery (Lead-acid and $LiFePO_4$), the three energy storage system controlled with the suggested strategy guarantees energy saving (respectively +15% with Lead-acid battery and +2.4% with $LiFePO_4$ battery), assures failsafe operations for the battery and FC unaffecting the drivability of the vehicle and increasing acceleration performance and autonomy.

References

[1] Tredeau, F.P.; Salameh, Z.M.; Evaluation of Lithium iron phosphate batteries for electric vehicles application, *Vehicle Power and Propulsion Conference, 2009. VPPC '09. IEEE*, 2009 , Page(s): 1266 – 1270.

[2] P. Harrop and R. Das, *Car Traction Batteries - the New Gold Rush 2010-2020*, IDTechEx report, 2009.

[3] Sadoun, R., Rizoug, N., Bartholomeus, P., Le Moigne, P., Optimal sizing of hybrid supply for electric vehicle using Li-ion battery and supercapacitor, (2014) *International Review of Electrical Engineering (IREE)*, 9 (2), pp. 332-340.

[4] Miller, J.M.; Energy storage system technology challenges facing strong hybrid, plug-in and battery electric vehicles, Vehicle Power and Propulsion Conference, 2009. VPPC '09. IEEE, 2009 , Page(s): 4 – 10.

[5] Isastia, V., Meo, S., Overview on automotive energy storage systems, (2009) *International Review of Electrical Engineering (IREE)*, 4 (6), pp. 1122-1144.

[6] Khaligh, A., Li, Z., Battery, Ultracapacitor, Fuel Cell, and Hybrid Energy Storage Systems for Electric, Hybrid Electric, Fuel Cell, and Plug-In Hybrid Electric Vehicles: State of the Art, Vehicular Technology, IEEE Transactions on, July 2010, Vol.: 59 Issue:6, page(s): 2806 – 2814.

[7] Ortuzar, M., Moreno, J., Dixon, J., Ultracapacitor-Based Auxiliary Energy System for an Electric Vehicle: Implementation and Evaluation, Industrial Electronics, IEEE Transactions on , vol.54, no.4, pp.2147-2156, Aug. 2007.

[8] Awerbuch, J.J., Sullivan, C.R., Control of Ultracapacitor-Battery Hybrid Power Source for Vehicular Applications, Energy 2030

Conference, 2008. ENERGY 2008. IEEE , vol., no., pp.1-7, 17-18 Nov. 2008.
[9] Eugenio Faggioli, Piergeorgio Rena, Veronique Danel, X. Andrieu, Ronald Mallant, Hans Kahlen, Supercapacitors for the energy management of electric vehicles, Journal of Power Sources, Volume 84, Issue 2, December 1999, Pages 261-269.
[10] Guidi, G., Kawamura, A., Efficient use of Electric Double Layer Capacitor as energy source on board of electric vehicles, Industrial Electronics (ISIE), 2010 IEEE International Symposium on, pp.3636-3641, 4-7 July 2010.
[11] Guiping Wang, Panpan Yang, Jinjin Zhang, Fuzzy optimal control and simulation of battery-ultracapacitor dual-energy source storage system for pure electric vehicle, Intelligent Control and Information Processing (ICICIP), 2010 International Conference on, pp.555-560, 13-15 Aug. 2010.
[12] Zhang Chenghui, Shi Qingsheng, Cui Naxin, Li Wuhua, Particle Swarm Optimization for energy management fuzzy controller design in dual-source electric vehicle, Power Electronics Specialists Conference, 2007. PESC 2007. IEEE, pp.1405-1410, 17-21 June 2007.
[13] S. Meo, F. Esposito, An Optimal Energy Management Strategy for Power-Split Hybrid Electric Vehicles, (2006) *International Review of Electrical Engineering (IREE)*, 1 (5), pp. 619-632.
[14] Kabisch, M., Heuer, M., Heideck, G., Styczynski, Z.A., Energy management of vehicle electrical system with auxiliary power unit, Vehicle Power and Propulsion Conference, 2009. VPPC '09. IEEE, pp.358-363, 7-10 Sept. 2009.
[15] Esposito, F., Isastia, V., Meo, S., PSO based energy management strategy for pure electric vehicles with dual energy storage systems, (2010) *International Review of Electrical Engineering (IREE)*, 5 (5), pp. 1862-1871.
[16] Zhi-Hui Zhan; Jun Zhang, Yun Li, Chung, H.S.-H., Adaptive Particle Swarm Optimization, Systems, Man, and Cybernetics, Part B: Cybernetics, IEEE Transactions on, vol.39, no.6, pp.1362-1381, Dec. 2009.
[17] I. C. Trelea, The particle swarm optimization algorithm: convergence analysis and parameter selection, Information Processing Letters, v.85 n.6, p.317-325, 31 March 2003.
[18] Esposito, F., Gentile, G., Isastia, V., Meo, S., A new bidirectional soft-switching multi-input DC-DC converter for automotive applications, (2010) *International Review of Electrical Engineering (IREE)*, 5 (4), pp. 1336-1346.
[19] ADVISOR® Data files.
[20] Boutte, A., Midoun, A., Identification of lead-acid battery parameters by Kalman filter using various battery models, (2014) *International Review of Automatic Control (IREACO)*, 7 (1), pp. 90-97.
[21] V. H. Johnson, Battery performance models in ADVISOR, Journal of Power Sources, Volume 110, Issue 2, 22 August 2002, Pages 321-329.
[22] Coman, P.T., Veje, C.T., Analysis and modeling of heat generation in overcharged Li-ion battery with passive cooling, (2013) *International Review of Mechanical Engineering (IREME)*, 7 (2), pp. 293-300.
[23] Brando, G.; Dannier, A; Spina, I; Piegari, L., "Comparison of accuracy of different LiFePO4 battery circuital models," Power Electronics, Electrical Drives, Automation and Motion (SPEEDAM), 2014 International Symposium on , vol., no., pp.1092,1097, 18-20 June 2014. doi: 10.1109/SPEEDAM.2014.6872021
[24] Laughton, M.A.: Fuel cells, Power Engineering Journal, Volume: 16 Issue: 1, Feb. 2002.
[25] U.S. Dept. of Energy – Nat.l Energy Techn. Lab., Fuel Cell Handbook (5th ed.), October 2000.
[26] Bucci, G.; Ciancetta, F.; Fiorucci, E.; Vegliò, F.: An Experimental Approach to the Modeling of PEM Fuel Cells in Dynamic Conditions; IEEE Powertech 2007, 1 - 5 July, Lausanne, Switzerland.
[27] Tiss, F., Ghabara, T., Chouikh, R., Guizani, A., A comprehensive CFD model of protonexchange membrane fuel cell, (2013) *International Review of Mechanical Engineering (IREME)*, 7 (7), pp. 1439-1445.
[28] Fei Gao ; Blunier, B. ; Miraoui, A. ; El Moudni, A., A Multiphysic Dynamic 1-D Model of a Proton-Exchange-Membrane Fuel-Cell Stack for Real-Time Simulation, Industrial Electronics, IEEE Transactions on, Publication Year: 2010 , Page(s): 1853 - 1864
[29] Sedghisigarchi, K. ; Davari, A. ; Famouri, P., Dynamic modeling and control of a fuel cell for electric vehicle applications, Vehicle Power and Propulsion Conference (VPPC), 2011 IEEE.
[30] Bucci, G.; Ciancetta, F.; Fiorucci, E.: An Automatic Test System for the Dynamic Characterization of PEM Fuel Cells, IEEE Instrumentation and Measurement Technology Conference, Como, ITALY, May 18-20, 2004.
[31] Baisden, A.C., Emadi, A., ADVISOR-based model of a battery and an ultra-capacitor energy source for hybrid electric vehicles, Vehicular Technology, IEEE Transactions on , vol.53, no.1, pp. 199- 205, Jan. 2004.
[32] S. Meo, F. Esposito, The "EVALUATOR" Suite for the Computer-aided Analysis of Advanced Automotive Electrical Power System, (2007) *International Review of Electrical Engineering (IREE)*, 2 (6), pp. 751-762.

Authors' information

Department of Electrical Engineering and information technology, Federico II University of Naples, 21 Claudio, 80125 Naples, Italy.
E-mail: santolo@unina.it

Andrea Del Pizzo, received the M.S. in Electrical Engineering in 1979 from the University of Naples (Italy). Here, he became assistant professor in 1983 and full professor of Electrical Machines and Drives in 2001; since 2003 he is president of Electrical Engineering Faculty. His main research fields of interest are modeling of electrical machines and drives, high performance PM brushless drives for electrical traction, power electronic transformer. Prof. Del Pizzo is IEEE member, and takes part in several scientific committees of international conferences.

Santolo Meo received B.S. and M.S. degrees with honours from FEDERICO II University of Naples - Italy, where currently he is an associate professor. He has actually three courses for students of Electrical and mechanical Engineering (Power Electronics, Power Electronics Laboratory and Railway Propulsion). His current research interests include the fields of power electronics and electrical drives. He is the author of about 100 scientific publications on journals and international conferences in the power electronics field. He is Editor-in-chief of the *International Review of Electrical Engineering (IREE)* and of the *International Review on Modelling and Simulations (IREMOS).* He is President of the Chapter Board on *Power Electronics and electrical drives* of the *World Scientific and Engineering Academy and Society*; he is member of the international scientific committee of International Conferences on Power electronics and control of electrical drives; he is reviewer for Journals and International Conferences on Power electronics and control of electrical drives; he was involved in National Research Projects financed by the Italian Minister of the Research; he has been responsible of several contracts of advice stipulated with the Researches Centre ELASIS of FIAT, on topics of power electronics for automotive applications.

Gianluca Brando was born in Naples, Italy, on September 27th 1973. He received the M.S. and the Ph.D. degrees both in Electrical Engineering from the University of Naples Federico II, respectively in 2001 and 2004. He is, at present, a post-doc research assistant at the Department of Electrical Engineering of the University of Naples Federico II. His main fields of interest are control technique of multilevel converter, control techniques of asynchronous machines and fault tolerance applied to converters.

Adolfo Dannier was born in Naples, Italy, on October 26th 1976. He received the M.S. and the Ph.D. degrees both in Electrical Engineering from the University of Naples Federico II, respectively in 2003 and 2008. He is, at present, a post-doc research assistant at the Department of Electrical Engineering of the University of Naples Federico II. His main fields of interest are multilevel converter, fault tolerance applied to converter, power electronic transformer and control of active front-ends.

Fabrizio Ciancetta was born in Pescara, Italy, in 1977 and he received the degree of electronic engineering in 2003 from the University of L'Aquila in Italy. In 2003 he joined the Department of Electrical Engineering of the University of L'Aquila as a part-time researcher on a research project aimed at the development of digital and distributed measurement system and measurement software optimization. In 2006 he received Ph.D. in electrical and information engineering at the same university. His current research interests include distributed measuring system, smart web sensors based on web service, virtual instrumentation, real-time measurement algorithms and devices, multiprocessor-based measuring systems. He has authored 70 scientific papers.

